Dalton Transactions



PAPER View Article Online View Journal



Cite this: DOI: 10.1039/c9dt02164g

Correlating magnetic anisotropy with [Mo(CN)₇]⁴⁻ geometry of Mn^{II}-Mo^{III} magnetic frameworks†‡

Four new three-dimensional (3-D) coordination frameworks based on the heptacyanomolybdate(III) anion were prepared and characterised by magnetic measurements: $\{[Mn^{II}(imH)_2]_2[Mn^{II}(H_2O)(imH)_3][Mn^{II}(imH)_4][Mo^{III}(CN)_7]_2 \cdot 6H_2O\}_n$ (1) (imH = imidazole), $\{[Mn^{II}(H_2O)_2(imH)]_3[Mn^{II}(H_2O)(imH)_2][Mo^{III}(CN)_7]_2 \cdot 5H_2O\}_n$ (2), $\{[Mn^{II}(Htrz)(H_2O)_2][Mn^{II}(Htrz)_{0.7}(H_2O)_{2.3}][Mo^{III}(CN)_7]_2 \cdot 5.6H_2O\}_n$ (3) (Htrz = 1,2,4-triazole) and $\{[Mn^{II}(H_2O)_2]_3[Mn^{II}(H_2O)_4][Mo^{III}(CN)_7]_2 \cdot 6H_2O \cdot 2urea\}_n$ (4). All four compounds exhibit long-range ferrimagnetic ordering and exhibit an opening of their magnetic hysteresis loops at 1.8 K; 1 and 2 exhibit the highest coercive fields among all known $[Mo^{III}(CN)_7]$ -based assemblies, 5000 and 4500 Oe respectively. The coercivity of 1–4 is correlated with the geometry of the heptacyanomolybdate(III) anion and the cyanide bridging pattern. A paramagnetic analogue of compound 1, $\{[Mn^{II}(imH)_2]_2[Mn^{II}(H_2O)(imH)_3][Mn^{II}(imH)_4][Re^{III}(CN)_7]_2 \cdot 6H_2O\}_n$ (1Re), where the heptacyanomolybdate(III) anion is substituted by the diamagnetic heptacyanorhenate(III) anion is also reported which constitutes the first example of a coordination framework based on $[Re^{III}(CN)_7]^{4-}$.

Received 22nd May 2019, Accepted 27th June 2019 DOI: 10.1039/c9dt02164g

Introduction

Magnetic coordination frameworks trace their origins to the discovery of Prussian Blue (PB) in 1706 in Berlin by the paint maker Diesbach while working in the laboratories of Dippel.¹ The magnetic properties of PB were first investigated at Bell laboratories by Holden *et al.* who reported it to be a "new low-temperature ferromagnet"² with a Curie temperature of 5.5 K. The mechanism of the ferromagnetic interactions in PB was identified as 'valence delocalisation'³ in agreement with the fact that it is a class II mixed valence compound according to the Robin–Day classification.⁴ Recent interest in this type of magnetic material has been fueled by the discovery of hexacyanometallate PB analogues that exhibit remarkably high magnetic ordering temperatures including [Cr^{III}(CN)₆]-based frameworks that are magnets above room temperature.⁵⁻⁷

In addition to octahedral homoleptic cyanometallates, hepta- and octacyanometallates^{8,9} of 4d and 5d metal ions are important building blocks for a host of materials. An excellent

example of this chemistry is the elaboration of magnetic frameworks of the type $\{[Mn^{II}(L)_x(H_2O)_y]_2[Mo^{III}(CN)_7]\}\cdot nH_2O(L)$ = ligand) which were found to exhibit substantial magnetic anisotropy^{10–13} owing to the geometry of the seven-coordinate pentagonal bipyramidal Mo^{III} ion. Since this pioneering work of Kahn and coworkers, numerous extended coordination assemblies based on the [Mo^{III}(CN)₇]⁴⁻ anion have been reported, 14-22 including examples that exhibit porosity 21,22 and chirality.22 Research efforts also have been directed at capitalizing on the magnetic anisotropy of [Mo^{III}(CN)₇]⁴⁻ for the design of discrete polynuclear molecules.²³⁻²⁵ The most exciting result in this vein is a linear Mn₂^{II}Mo^{III} trinuclear molecule which exhibits the highest spin reversal barrier among all cyanide-bridged single molecule magnets. 24,25 This remarkable SMM behaviour,²⁶ including hysteresis at temperatures up to 3.2 K, is attributed to anisotropic superexchange interactions between metal spin centers in the Mo^{III}-CN-Mn^{II} linkage.²⁷⁻³⁰ which is also operative in the extended structures of $[Mo^{III}(CN)_7]^{4-}$ that exhibit wide magnetic hysteresis loops. ^{20,31}

Herein we report four new $Mn^{II}-Mo^{III}$ 3-D ferrimagnetically ordered coordination frameworks that exhibit high magnetic anisotropies. The compounds $\{[Mn^{II}(imH)_2]_2[Mn^{II}(H_2O)(imH)_3][Mn^{II}(imH)_4][Mo^{III}(CN)_7]_2 \cdot 6H_2O\}_n$ (1) (imH = imid-azole), $\{[Mn^{II}(H_2O)_2(imH)]_3[Mn^{II}(H_2O)(imH)_2][Mo^{III}(CN)_7]_2 \cdot 5H_2O\}_n$ (2), $\{[Mn^{II}(Htrz)(H_2O)_2][Mn^{II}(Htrz)_{0.7}(H_2O)_{2.3}][Mo^{III}(CN)_7]_5 \cdot 6H_2O\}_n$ (3) (Htrz = 1,2,4-triazole) and $\{[Mn^{II}(H_2O)_2]_3[Mn^{II}(H_2O)_4][Mo^{III}(CN)_7]_2 \cdot 6H_2O \cdot 2urea\}_n$ (4) were prepared and fully characterized. Compounds 1 and 2 are particularly notable in that they exhibit the largest coercive fields among heptacyanomolybdate(III) containing frameworks.

^aFaculty of Chemistry, Jagiellonian University, Gronostajowa 2, 30-387 Kraków, Poland. E-mail: dawid.pinkowicz@uj.edu.pl

^bDepartment of Chemistry, Texas A&M University, College Station, Texas 77843, USA. E-mail: dunbar@chem.tamu.edu

[†]This paper is dedicated to Annie Powell on the occasion of her 60th birthday for her major contributions to the field of molecular magnetism.

[‡] Electronic supplementary information (ESI) available: Additional structural diagrams and plots with PXRD, IR, and magnetic data. CCDC 1899234-1899238. For ESI and crystallographic data in CIF or other electronic format see DOI: 10.1039/c9dt02164g

Dalton Transactions Paper

Experimental section

Synthetic procedures

All manipulations were performed in a glovebox under an argon atmosphere unless stated otherwise. The precursor K₄[Mo^{III}(CN)₇]·2H₂O was prepared by a modified procedure described in the literature32 which involves the use of MoCl₃(THF)₃ instead of K₂MoCl₆. Distilled water was deoxygenated by refluxing for 12 hours under an argon atmosphere. All other reagents were analytical grade as supplied from commercial sources (Sigma-Aldrich, Alfa Aesar, Acros Organics).

K₄[Re^{III}(CN)₇]·2H₂O

The compound was prepared according to a modified literature procedure.33 Under ambient conditions, KCN (4.00 g, 61.0 mmol) was dissolved in 10 mL of H₂O which had not been deoxygenated and ReCl₃ (0.59 g, 2.0 mmol) was slowly added. The solution was stirred for 2 hours and then refluxed for 12 hours under a flow of argon, resulting in a brown mixture that was sealed under argon and filtered to remove a purple impurity. The mixture was treated dropwise with 15 mL of deoxygenated methanol which produced a yellowish solid. After filtration, a creamy-yellow solid was collected which was dried for 15 minutes under vacuum. Yield: 0.88 g (75%). EA Found: C, 14.69; H: 1.03; N, 17.15; calculated for K₄[Re^{III}(CN)₇]·2H₂O: C, 14.99; H: 0.72; N: 17.48. IR (cm⁻¹): 3613s, 3569m, 3500m, 3430m(br), 3222w, 2125m, 2113m, 2101s, 2092vs, 2070s, 2039vs, 2004m, 1627m (Fig. S1 and S2 in the ESI‡).

 ${[Mn^{II}(imH)_{2}]_{2}[Mn^{II}(H_{2}O)(imH)_{3}][Mn^{II}(imH)_{4}][Mo^{III}(CN)_{7}]_{2}}$ $6H_2O_{n}$ (1). Anhydrous MnCl₂ (32 mg, 0.25 mmol) and imidazole (360 mg, 5.29 mmol) were dissolved in 20 mL of H₂O and added dropwise to a solution of K₄[Mo^{III}(CN)₇]·2H₂O (34 mg, 0.07 mmol) in 20 mL of H₂O. Over the course of 12 h, large green needle crystals formed and were collected by decanting the solution. Yield: 30 mg (52%). EA Found: C, 34.49; H, 3.38; N, 30.71; calculated for $[Mn^{II}(imH)_2]_2$ [Mn^{II}(H₂O)(imH)₃][Mn(imH)₄] [Mo^{III}(CN)₇]₂·6H₂O: C, 34.20; H, 3.54; N, 30.54. IR (cm⁻¹): 3402s, 3231s(br), 3140s, 3067m, 2956m, 2864m, 2160w, 2113s, 2050m, 1621m(br), 1537m, 1489m, 1423m, 1326m, 1257m, 1166w, 1134w, 1098w, 1065s (Fig. S3a in the ESI‡).

 ${[Mn^{II}(H_2O)_2(imH)]_3[Mn^{II}(H_2O)(imH)_2][Mo^{III}(CN)_7]_2 \cdot 5H_2O}_n$ (2). Samples of anhydrous MnCl₂ (28 mg, 0.22 mmol) and imidazole (50 mg, 0.74 mmol) were dissolved in 12 mL of H₂O and the solution was added dropwise to K₄[Mo^{III}(CN)₇]·2H₂O (24 mg, 0.05 mmol) in 8 mL of H₂O. After several hours, green prism crystals had formed and were collected by decantation. Yield: 10 mg (30%). EA Found: C, 26.55; H, 2.99; N, 25.63; calculated for $[Mn^{II}(H_2O)_2(imH)]_3[Mn^{II}(H_2O)(imH)_2[Mo^{III}(CN)_7]_2$. 5H₂O: C, 26.14; H, 3.33; N, 25.23; small discrepancies between the predicted and observed composition are attributed to partial loss of water of crystallization. IR (cm⁻¹): 3601s, 3373vs (br), 3138s, 2143m, 2113s, 2094s, 1615m(br), 1533w, 1509w, 1490w, 1422w, 1327w, 1255w, 1164w, 1128w, 1098w, 1068s (Fig. S3b‡).

 ${[Mn^{II}(Htrz)(H_2O)_2][Mn(Htrz)_{0.7}(H_2O)_{2.3}][Mo^{III}(CN)_7] \cdot 5.6H_2O}_n$ (3). Quantities of anhydrous MnCl₂ (21 mg, 0.17 mmol) and 1,2,4-triazole (67 mg, 0.97 mmol) were dissolved in 6 mL of H₂O and added dropwise to a solution of K₄[Mo^{III}(CN)₇]·2H₂O (24 mg, 0.05 mmol) in 6 mL of H₂O. A green precipitate formed after several hours which redissolved; large dark-green blocks crystallized within three days which were collected by decantation. Yield: 15 mg (44%). EA Found: C, 20.76; H, 2.85; N, 28.53; calculated for $\{[Mn^{II}(Htrz)(H_2O)_2][Mn^{II}(Htrz)_{0.7}\}$ $(H_2O)_{2,3}$ $[MO^{III}(CN)_7] \cdot H_2O\}_n$: C, 20.78; H, 2.62; N, 28.22; crystals of 3 lose water instantaneously when removed from the mother liquid which leads to a major difference between the number of interstitial H2O molecules located by the X-ray data and the number calculated from the EA. IR (cm^{-1}) : 3606s, 3378s(br), 2143m, 2216s, 2081s, 1615m(br), 1377w, 1297w, 1159w, 1068w, 988w (Fig. S3c‡).

 ${[Mn^{II}(H_2O)_2]_3[Mn^{II}(H_2O)_4][Mo^{III}(CN)_7]_2 \cdot 6H_2O \cdot 2urea}_n$ (4). Anhydrous MnCl₂ (92 mg, 0.73 mmol) and urea (350 mg, 5.83 mmol) were dissolved in 7 mL of H₂O and added dropwise to a solution of K₄[Mo^{III}(CN)₇]·2H₂O (42 mg, 0.09 mmol) and urea (420 mg, 7.00 mmol) in 6.5 mL of H₂O. Large green columnar crystals appeared after 12 h and were collected by decantation. Yield: 25 mg (47%). EA Found: C, 16.01; H: 3.31; N, 21.02; calculated for $[Mn^{II}(H_2O)_2]_3[Mn^{II}(H_2O)_4][Mo^{III}(CN)_7]_2$. 6H₂O·2urea: C, 16.23; H, 3.40; N, 21.29. IR (cm⁻¹): 3485vs, 3374vs, 3340vs(br), 2139m, 2115m, 2084vs, 2060s, 1621s, 1558m, 1489m, 1136w (Fig. S3d‡).

 ${[Mn^{II}(imH)_{2}]_{2}[Mn^{II}(H_{2}O)(imH)_{3}[Mn^{II}(imH)_{4}][Re(CN)_{7}]_{2}\cdot6H_{2}O}_{n}$ (1Re). Anhydrous MnCl₂ (32 mg, 0.25 mmol) and imidazole (360 mg, 5.29 mmol) were dissolved in 20 mL of H₂O and added dropwise to a solution of K₄[Re^{III}(CN)₇]·2H₂O (41 mg, 0.07 mmol) in 20 mL of H2O. Large dark yellow needles formed over the period of 12 h and were collected by decantation. Yield: 30 mg (47%). EA Found: C, 31.26; H, 2.95; N, 27.91; calculated for $[Mn^{II}(imH)_2]_2[Mn^{II}(H_2O)(imH)_3][Mn^{II}(imH)_4]$ $[Re^{III}(CN)_7]_2 \cdot 6H_2O$: C, 30.82; H, 3.19; N, 27.53. The small discrepancy between predicted and observed values is attributed to partial loss of water of crystallization. The purity of the sample was also confirmed by powder X-ray diffraction (Fig. S5 in the ESI $^{+}$). IR (cm⁻¹): 3607s, 3406vs, 3140vs(br), 2956vs, 2852vs, 2711s, 2617s, 2547m, 2508m, 2382w, 2321w, 2146s, 2119vs, 2095vs, 2055vs, 1618s(br), 1532s, 1491s, 1420s, 1324s, 1282w, 1259s, 1205w, 1173m, 1158w, 1141m, 1127w, 1102s, 1089s, 1060vs (Fig. S4‡).

Results and discussion

Crystal structures

 ${[Mn^{II}(imH)_{2}]_{2}[Mn^{II}(H_{2}O)(imH)_{3}][Mn^{II}(imH)_{4}][Mo^{III}(CN)_{7}]_{2}}$ $6H_2O_{n}$ (1). Compound 1 crystallises in the centrosymmetric monoclinic C2/c space group with the asymmetric unit consisting of one Mo^{III} ion and three types of Mn^{II} centres, with Mn1 lying on a c glide plane and the Mn3 atom residing on a twofold symmetry axis (see Fig. S6 in the ESI‡). The Mn1 atom is bound to four imidazole equatorial ligands and two axial

N-bonded CN groups, resulting in a slightly distorted octahedron. The Mn2 centre adopts a distorted trigonal bipyramidal geometry with two imidazole and three cyanide ligands. The Mn3 site is similar to that of Mn1, but with one imidazole ligand being substituted by a coordinated water molecule.

Dalton Transactions

The $[Mo^{III}(CN)_7]^{4-}$ anion in 1 adopts a nearly ideal pentagonal bipyramidal geometry and engages in one axial and four equatorial cyanide bridges to the Mn ions (Fig. 1a). Three equatorial bridges are very similar, with Mo1-Mn2 separations ranging from 5.433 Å to 5.454 Å, whereas Mo1-Mn3 and axial Mo1-Mn1 distances are significantly shorter (5.316 Å and 5.331 Å respectively) which is ascribed to the more pronounced bending of the C-N-Mn units. These structural features result in a complex 3-D coordination network. Along the c crystallographic axis, the bonding pattern involves square-like and circular motifs which lead to the appearance of tubular channels along the c axis (Fig. 2a) which are occupied by water molecules.

 ${[Mn^{II}(H_2O)_2(imH)]_3[Mn^{II}(H_2O)(imH)_2][Mo^{III}(CN)_7]_2 \cdot 5H_2O_{ln}}(2).$ The crystal structure of compound 2 was solved in the $P\bar{1}$ space group with two inequivalent MnII sites residing in the asymmetric unit (Fig. S7 in the ESI‡). The coordination sphere of one of the Mn atoms is composed of an imidazole molecule, two H₂O ligands in a cis geometry and three nitrogen atoms in a mer arrangement belonging to cyanide ligands from different $[Mo^{III}(CN)_7]^{4-}$ anions. The octahedral geometry of this centre is substantially distorted as evidenced by the O-Mn-O angle of 74.4(4)°. The second Mn^{II} center is similar to the first one, but one of its coordination sites is equally occupied by an aqua ligand plus one crystallization water molecule or an imidazole ligand. This disorder is likely due to scrambling of [Mn^{II}(H₂O)₂(imidazole)] and [Mn^{II}(H₂O)(imidazole)₂] moieties in the Mn2 position which means that the unit cell lacks inversion centre symmetry and pairs of symmetry equivalent Mn2 sites do not consist of two identical moieties.

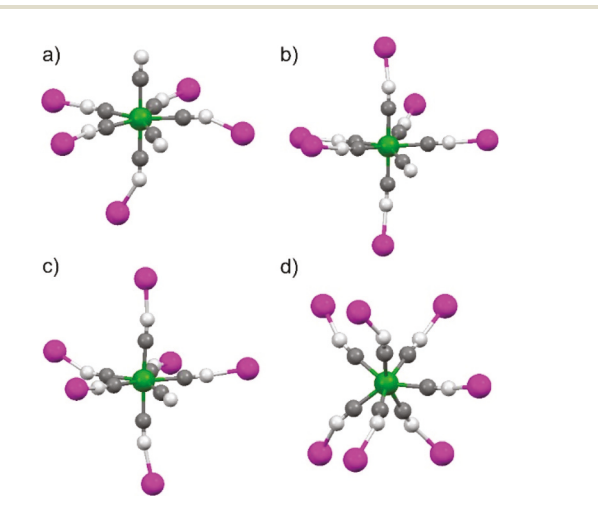


Fig. 1 Heptacyanomolybdate(III) coordination environment in compounds 1-4 (a-d respectively); Mo - green, Mn - magenta, C - grey, N white.

The [Mo^{III}(CN)₇]⁴⁻ anion in 2 is in a distorted pentagonal bipyramidal geometry (Fig. 1b) with six of the seven cyanide ligands engaged in bridging interactions with MnII centres. This leads to the formation of a 3-D crossed-ladder topology (Fig. 2b), similar to the $\{[Mn^{II}(H_2O)_2(imH)]_2[M^{IV}(CN)_8]\cdot 4H_2O\}_n$ networks based on octacyanometallates (M = Nb, 34 Mo, 35 W 36) in spite of the higher imidazole content. Appearance of a structural disorder involving the additional imidazole molecule in 2 is likely related to the "missing cyanide" of the [Mo^{III}(CN)₇]⁴⁻ as compared to the analogous $[M^{IV}(CN)_8]^{4-}$ compounds. $^{34-36}$

 ${[Mn^{II}(Htrz)(H_2O)_2][Mn(Htrz)_{0.7}(H_2O)_{2.3}][Mo^{III}(CN)_7] \cdot 5.6H_2O}_n$ (3). Compound 3 crystallizes in the $P\bar{1}$ space group. The asymmetric unit is composed of two Mn^{II} cations and one $[Mo^{III}(CN)_7]^{4-}$ anion (Fig. S8 in the ESI‡). Mn1 is connected to three nitrogen atoms of $[Mo^{III}(CN)_7]^{4-}$ in a mer configuration and two oxygen atoms of H2O ligands in a trans disposition. The coordination sphere is completed by a nitrogen atom from a disordered 1,2,4-triazole molecule. The best refinement was obtained for a ligand occupancy of 70%, with the remaining 30% corresponding to three hydrogen-bonded water molecules, one of which is coordinated to MnII. This composition was confirmed by elemental analysis (see Experimental section). The environment of Mn2 is similar to Mn1 except the coordinated H2O molecules are cis to each other and there is no disorder associated with the 1,2,4-triazole ligand.

The [Mo^{III}(CN)₇]⁴⁻ anion in 3 is only slightly distorted from an ideal pentagonal bipyramid (Fig. 1c). As in the case of 2, there are six cyanide bridges and one terminal equatorial cyanide which leads to nearly identical topologies (as depicted in Fig. 2b and 2c). One of the equatorial Mo^{III}-C-N-Mn^{II} cyanide bridges in 3, however, is significantly more bent at 156.7(3)° vs. 174.5(5)° while both axial bridges are closer to linear as compared to 2 (3: 170.6(3)° and 169.3(3)° vs. 2: 163.2(5)° and 160.1(5)°; see Fig. S10 in the ESI‡). Both networks in 2 and 3 are characterised by a loosely packed structure, rendering the crystals susceptible to water loss.

 ${[Mn^{II}(H_2O)_2]_3[Mn^{II}(H_2O)_4][Mo^{III}(CN)_7]_2 \cdot 6H_2O \cdot 2urea}_n$ (4). Crystals of 4 belong to the P1 triclinic space group with a unit cell that consists of two asymmetric units composed of [Mo^{III}(CN)₇]⁴⁻ and four Mn^{II} centres located at special positions (Fig. S9 in the ESI‡). Three Mn^{II} ions adopt similar coordination geometries with two trans H2O ligands and four equatorially N-bonded cyanides. The fourth MnII ion is bound to four water molecules located in equatorial positions and two N atoms of trans CN ligands. The unit cell also contains six outer-sphere water molecules and two urea molecules per Mn₄Mo₂ unit. Each urea molecule is engaged in three hydrogen bonds to the carbonyl oxygen atom with the neighbouring water molecules coordinated to Mn^{II}.

Compound 4 exhibits a complex 3-D cyanide-bridged coordination network in which each heptacyanomolybdate(III) unit forms seven cyanide bridges to Mn^{II} centres (Fig. 1d). The coordination sphere of the Mo^{III} ion is intermediate between a capped trigonal prism and a capped octahedron. A fragment of the structure is depicted in Fig. 2d.

Paper Dalton Transactions

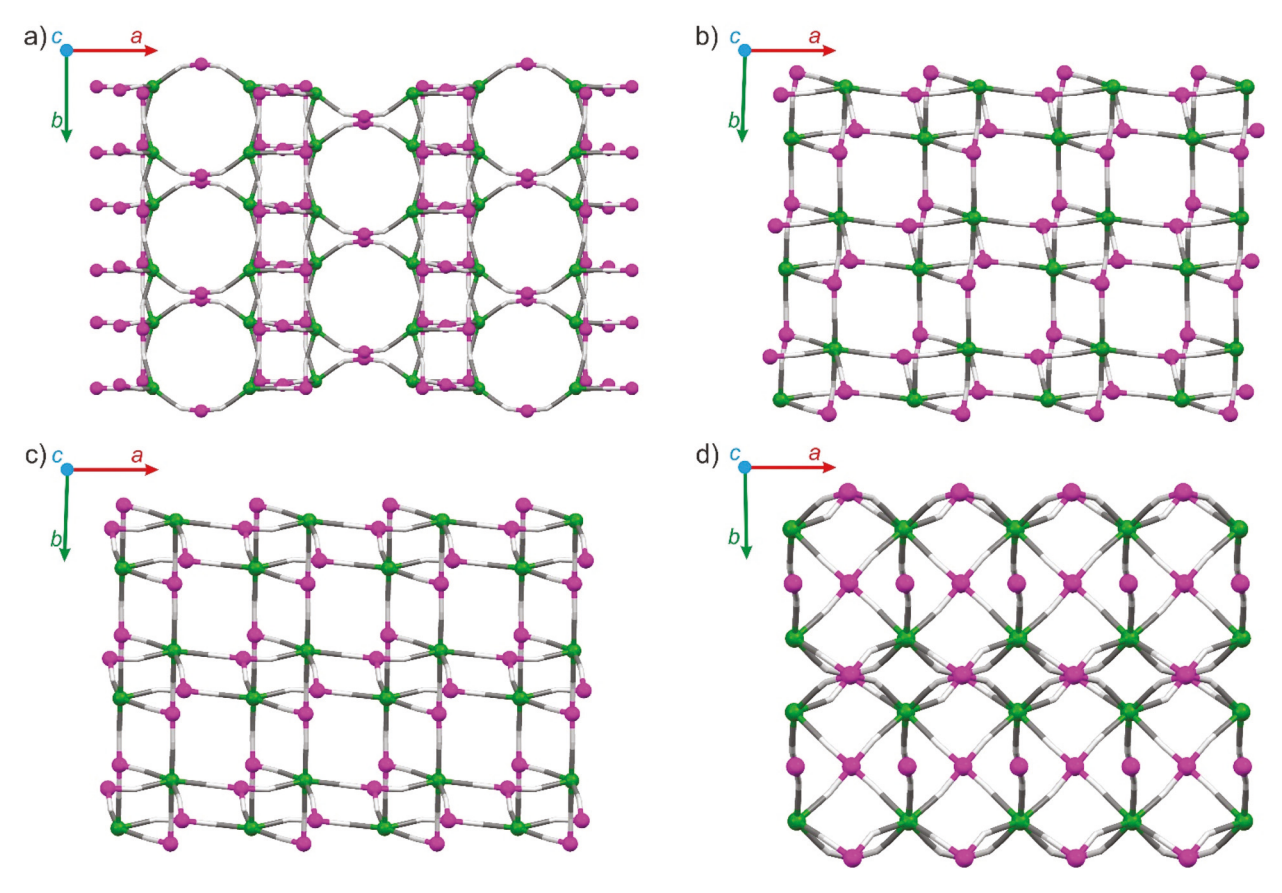


Fig. 2 Coordination skeletons of compounds (a) 1, (b) 2, (c) 3 and (d) 4 along the c axis. Organic ligands, water molecules and non-bridging cyanides were omitted for the sake of clarity. Mo – green, Mn – magenta, C – grey, N – white.

The most important structural features in terms of the magnetic properties of 1–4, namely the number of bridging cyanides and the geometry of the $[\mathrm{Mo^{III}(CN)_7}]^{4-}$ anions, are summarized in Table 1 along with previously crystallographically characterized $\mathrm{Mn^{II}_{-Mo^{III}(CN)_7}}$ compounds. These structural data are correlated with the temperature of the long range magnetic ordering $T_{\rm c}$ and the coercive field. Additional important crystal data and metrical parameters for compounds 1–4 are compiled in Tables S1 and S2.‡

 $\{[\mathbf{Mn^{II}}(\mathbf{imH})_2]_2[\mathbf{Mn^{II}}(\mathbf{H}_2\mathbf{O})(\mathbf{imH})_3][\mathbf{Mn^{II}}(\mathbf{imH})_4][\mathbf{Re^{III}}(\mathbf{CN})_7]_2$. $6\mathbf{H}_2\mathbf{O}\}_n$ (1Re). Compound 1 and its heptacyanorhenate(III)-based analogue 1Re are isomorphous (see structural diagrams in Fig. S11‡ and the powder X-ray diffraction patterns in Fig. S5‡). Stronger π -backbonding for the d^4 $[\mathrm{Re^{III}}(\mathbf{CN})_7]^{4-}$ anion as compared to the d^3 $[\mathrm{Mo^{III}}(\mathbf{CN})_7]^{4-}$ analogue leads to a shortening of the average M–C distance from 2.141(15) Å for $\mathrm{Mo^{III}}$ to 2.094(16) Å for $\mathrm{Re^{III}}$. There is only a small difference in the average Mn–N bond distances in 1Re (2.21(3) Å) and 1 (2.19(2) Å). The C–N–Mn angles (Table S2‡) are also similar in both compounds. Average M····Mn distances are 5.39(6) Å for 1 and 5.35(5) Å for 1Re, an indication that the framework adjusts to the varying sizes of the heptacyanometallate units rendering it adequate for diamagnetic dilution.

Magnetic properties

Compounds 1–4 are paramagnetic at temperatures higher than 29 K (1), 45 K (2 and 3) and 59 K (4). Experimental values of χT versus T at 250 K are 8.94 cm³ K mol⁻¹ for 1, 9.14 cm³ K mol⁻¹ for 2, 9.04 cm³ K mol⁻¹ for 3 and 8.96 cm³ K mol⁻¹ for 4 (see Fig. S12 in the ESI⁺₂), which are close to the expected spin-only value of 9.13 cm³ K mol⁻¹ per Mn₂Mo formula unit. Small discrepancies are attributed to deviations of the g factor of Mo^{III} from 2.0⁴¹ and antiferromagnetic interactions between Mo^{III} and Mn^{II} spin centers.

Compounds 1–4 exhibit a magnetic phase transition to a ferrimagnetic state as evidenced by an abrupt increase of the FC (field-cooled) magnetization and bifurcation of the ZFC/FC (zero field-cooled/field-cooled) at the critical temperatures of 29 K for 1, 45 K for 2 and 3 and 59 K for 4 (Fig. 3). These $T_{\rm c}$ values are in accord with the position of the χ' peak in the AC (alternating current) molar magnetic susceptibility data (Fig. S13a–d‡). The higher $T_{\rm c}$ values across the series are consistent with the increasing number of bridging cyanides per [Mo^{III}(CN)₇]^{4–} moiety (see Table 1 for reference). It is noted that compounds 2 and 3 with identical crossed-ladder topologies order magnetically at the same temperature of 45 K.

Table 1 Selected structural and magnetic data for Mn^{II}-[Mo^{III}(CN)₇] assemblies

	No. of contlete later	No. of cyanide bridges formed by [Mo ^{III} (CN) ₇] ⁴⁻		Comments	<i>m</i>		
$Compound^a$	No. of cyanide bridges formed by Mn(II)	Axial	Equatorial	Geometry of $[Mo^{III}(CN)_7]^{4-}$	T _c (K)	$H_{\rm c}\left({\rm Oe}\right)^b$	Ref.
1	2,2,3	1	4	PBPY^i	29	5000 ^(1.8 K)	This work
2	3	2	4	PBPY	45	4500 ^(1.8 K)	This work
$(NH_4)_3[(H_2O)Mn_3(HCOO)][Mo(CN)_7]_2 \cdot 4H_2O$	4,5,5	2	5	$JPBPY^j$	70	1500 ^(2 K)	20
$[Mn(dpop)]_2[Mo(CN)_7] \cdot 2H_2O^c$	2	1	2	PBPY	5.6	$1150^{(2 \text{ K})}$	31
$Mn_2(3-pypz)(H_2O)(CH_3CN)[Mo(CN)_7]^d$	3,4	7		$CTPR^k$	64	820 ^(2 K)	37
3	3	2	4	PBPY	45	710 ^(1.8 K)	This work
$[Mn(dpop)]_2[Mo(CN)_7] \cdot 2H_2O^c$	2	2	2	PBPY	25	305 ^(1.8 K)	38
$[Mn(dpop)]_3[Mn(dpop)(H_2O)][Mo(CN)_7]_2 \cdot 13.5H_2O^c$	1,2	1,2	2,2	PBPY	3	90 ^(1.8 K)	38
$[N(CH_3)_4]_2[Mn(H_2O)]_3[Mo(CN)_7]_2 \cdot 2H_2O$	4	6		COC^{l}	86	200 ^(1.8 K)	15
$[Mn(HL)(H_2O)]_2Mn[Mo(CN)_7]_2 \cdot 2H_2O^e$	4	6		COC	85	150 ^(2 K)	22
$Mn_2(pyim)(H_2O)(CH_3CN)[Mo(CN)_7]^f$	3,4	7		CTPR	62	146 ^(2 K)	37
$K_2Mn_3(H_2O)_6[Mo(CN)_7]_2 \cdot 6H_2O^b$	4	7		CTPR	39	125 ^(5 K)	14
4	2,4,4,4	7		CTPR/COC	59	110 ^(1.8 K)	This work
$Mn_2(1-pypz)(H_2O)(CH_3CN)[Mo(CN)_7]^g$	3,4	7		CTPR	66	$72^{(2 \text{ K})}$	37
$[Mn_2(tea)Mo(CN)_7] \cdot H_2O^h$	3,4	7		CTPR	75	70 ^(5 K)	17
$K_2(H_2O)_4Mn_5(H_2O)_8(MeCN)[Mo(CN)_7]_3 \cdot 2H_2O$	3,4,4,4,5	7,6,7		PBPY/CTPR	61	$70^{(2 \text{ K})}$	21
Mn ₂ [Mo(CN) ₇](pyrimidine) ₂ ·2H ₂ O	3,4	7		COC	47	$60^{(2 \text{ K})}$	19
$\{[Mn(dpop)]_4[(dpop)Mn(H_2O)]_2[Mo(CN)_7]_3 \cdot 27H_2O\}_n^b$	1,2	2,2,2	0,2,2	PBPY	2.2	$30^{(1.8 \text{ K})}$	39
$[NH_4]_2Mn_3(H_2O)_4[Mo(CN)_7]_2 \cdot 4H_2O$	4,5,5	7		COC/CTPR	53	$0^{(1.8K)}$	18
$Mn_2(H_2O)_5[Mo(CN)_7]\cdot 4H_2O(\alpha \text{ phase})^m$	3,4	7		CTPR	51	0 ^(5 K)	11
$Mn_2(H_2O)_5[Mo(CN)_7]\cdot 4.75H_2O(\beta \text{ phase})^m$	3,4	7		CTPR	51	$0^{(5 \text{ K})}$	12

 $[^]a$ All assemblies exhibit 3-D connectivity except $K_2Mn_3(H_2O)_6[Mo(CN)_7]_2 \cdot 6H_2O$ and $\{[Mn(dpop)]_4[(dpop)Mn(H_2O)]_2[Mo(CN)_7]_3 \cdot 27H_2O\}_n$. b Values listed in brackets represent temperatures at which hysteresis loops were recorded. c dpop = 2,13-dimethyl-3,6,9,12,18-pentaazabicyclo[12.3.1]-octadeca-1(18),2,12,14,16-pentaene. d 3-pypz = 2-(1H-pyrazol-3-yl)pyridine. e L = N,N-dimethylalaninol. f pyim = 2-(1H-imidazol-2-yl)pyridine. f Tea = triethanolamine. f PBPY = pentagonal bipyramid. f JPBPY = Johnson pentagonal bipyramid. k CTPR = capped trigonal prism. ⁷COC = capped octahedron. ^mWhile authors report both phases to be distorted pentagonal bipyramids, quantitative estimation of the geometry using SHAPE software⁴⁰ leads to the distorted capped trigonal prism.

The M(H) curves for all four compounds exhibit magnetic hysteresis at 1.8 K (Fig. 4 and Table 1). In the case of 1, the coercive field (H_c) is 5000 Oe with a remnant magnetisation M_r of 3.8 $N\beta$ and for 2 H_c = 4500 Oe and M_r = 4.3 $N\beta$. For 3 and 4 the hysteresis loops are narrower at 710 and 110 Oe and the remnant magnetization values are 3.6 and 1.2 $N\beta$, respectively. Of particular note is the fact that 1 and 2 exhibit coercivities of 5000 and 4500 Oe, respectively which are the largest reported values for heptacyanomolybdate(III) containing compounds. The H_c values are independent of the grain shape or size as the samples of 1-4 are all crystalline (0.2 mm monocrystals) with no visible grain boundaries, in contrast to metal alloys or ceramic magnets produced by sintering of metal oxides. Given the absence of other magnetically anisotropic building blocks, the coercivity properties of $\{[Mn^{II}(L)_x(H_2O)_y]_2\}$ $[Mo^{III}(CN)_7]$ $\cdot nH_2O$ magnets emanate from the orbitally degenerate $S = \frac{1}{2}$ pentagonal bipyramidal $[Mo^{III}(CN)_7]^{4-}$ anion which engages in anisotropic exchange interactions. ^{27–30} The widest magnetic hysteresis loop was observed for 1 whose structure is closest to an ideal pentagonal bipyramid (PBPY) (see Table S1‡). One might expect 3 to exhibit the coercivity similar to 1 given that the Mo^{III} unit is only slightly more distorted from pentagonal bipyramidal geometry, but the H_c value is only 710 Oe as compared to 5000 Oe for 1. In addition, this value is actually seven times less than that of 2 (4500 Oe) in spite of the fact that the [Mo^{III}(CN)₇]⁴⁻ anion in 2 is significantly more distorted from an ideal PBPY. The main structural differences between 2 and 3 are less bent apical C-N-Mn angles in 3 and a significant bending of the equatorial C-N-Mn bridge in 3 (156.7(3)°) as compared to 2 (174.5(5)°; Fig. S10 and Table S2 in the ESI‡). These metrical differences directly impact orbital overlap hence magnetic exchange interactions as well as orientations of the anisotropy axis associated with the [Mo^{III}(CN)₇]⁴⁻ moiety.³⁰

The coercive field of 110 Oe exhibited by 4 indicates a small magnetic anisotropy, typical of heptacyanomolybdate(III) assemblies with large deviations from a pentagonal bipyramidal geometry. An analysis of the coercivities and the geometry of the $[Mo^{III}(CN)_7]^{4-}$ bridging unit for the compounds in Table 1 reveals that a pentagonal bipyramidal geometry is a necessary, but not sufficient, criterion for wide magnetic hysteresis loops.

The M(H) curves at 7 T reach values of 7.55 $N\beta$ for 1, 8.10 N β for 2, 8.99 N β for 3 and 8.98N β for 4, approaching the expected 9.0 $N\beta$ for antiferromagnetically coupled Mn₂Mo units. It is worth mentioning that the magnetization data for 1 and 2 do not saturate (Fig. S14 in the ESI‡) which is another indication of substantial magnetic anisotropy, as even a strong magnetic field of 7 T is insufficient to completely align magnetic domains.

Given its large H_c value, compound 1 is a good candidate for introducing SMM-like behaviour via diamagnetic dilution

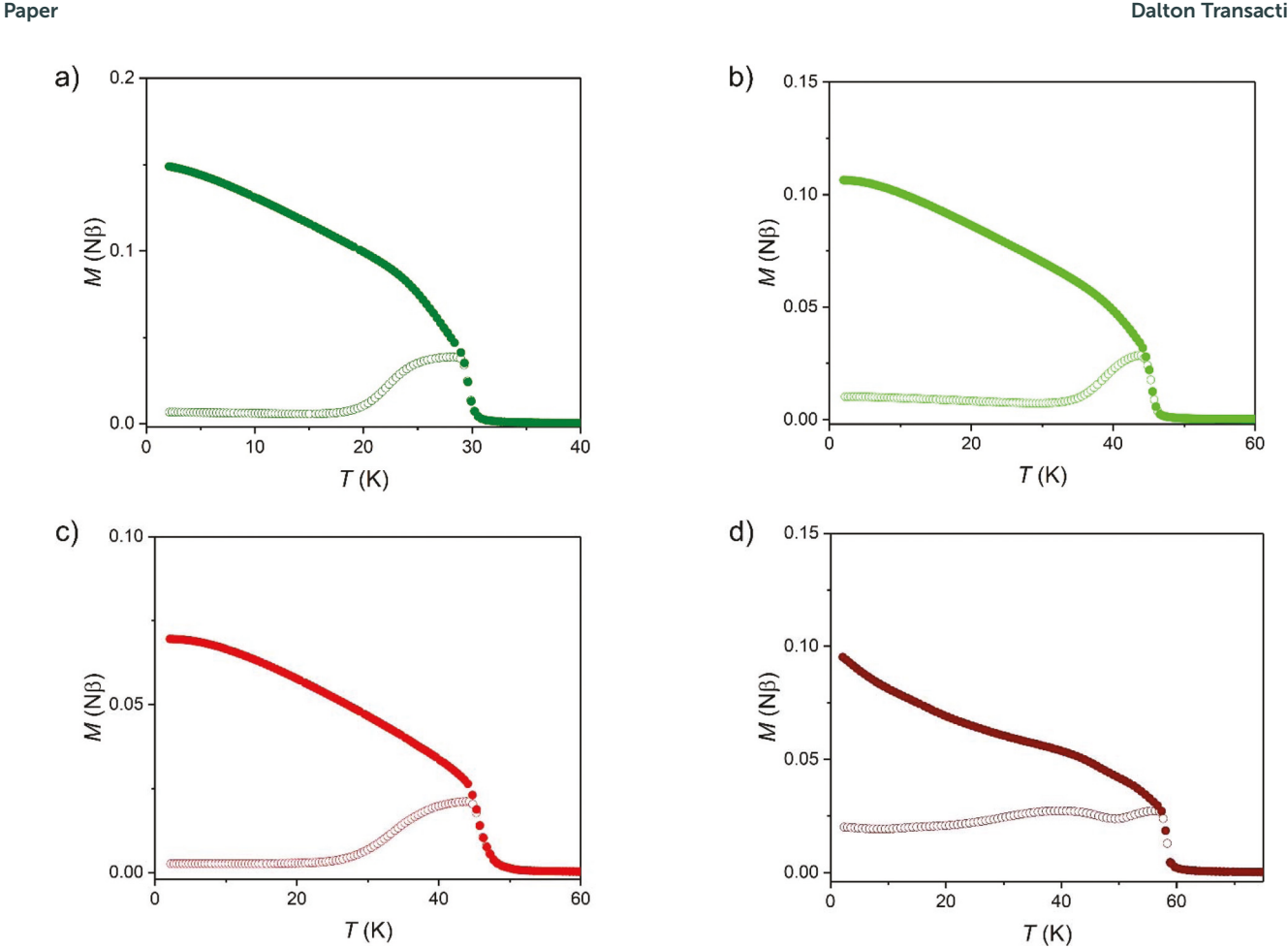


Fig. 3 Zero field-cooled (open circles) and field-cooled (full circles) M(T) plots for compounds 1–4 (a–d respectively) at H_{DC} = 3 Oe.

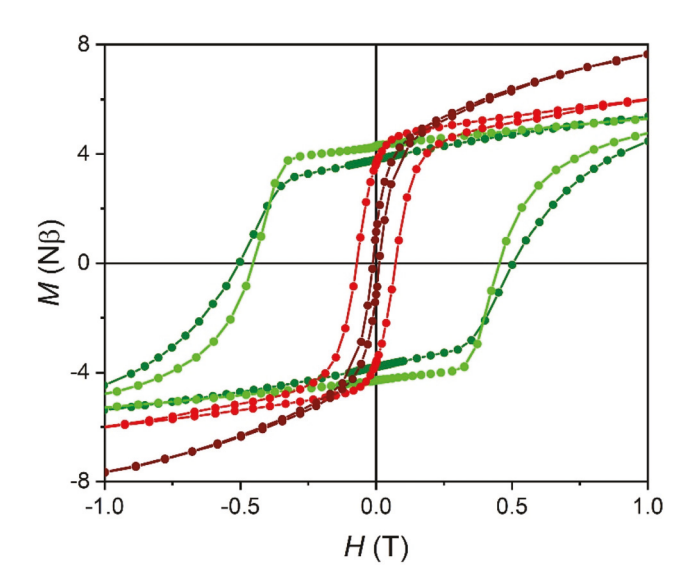


Fig. 4 Magnetisation versus magnetic field plots for compounds 1 (dark green), 2 (green), 3 (red) and 4 (dark red) at T = 1.8 K. Solid lines are guides for the eye.

using $[Re^{III}(CN)_7]^{4-}$. Our attempt to synthesize the structural analogue of 1 was successful and led to the isolation ${[Mn^{II}(imH)_{2}]_{2}[Mn^{II}(H_{2}O)(imH)_{3}][Mn^{II}(imH)_{4}][Re^{III}(CN)_{7}]_{2}}$ $6H_2O_{n}^{1}$ (1Re). The compound is a simple paramagnet with very weak antiferromagnetic interactions between the Mn^{II} ions, separated by the diamagnetic Re^{III} centers. The magnetic data were modelled by using the mean-field approximation implemented in the PHI software, 42 and fitting of $\chi T(T)$ curve was performed with the following expression:

$$\chi = \chi_{\rm calc} / [1 - (zJ/N_{\rm A}\mu_{\rm B}^2)\chi_{\rm calc}] \tag{1}$$

which yields $g_{\text{Mn}} = 2.02(5)$ and zJ = -0.05(1) cm⁻¹ (Fig. S15 in the ESI‡). The magnetization data at 7 T and 2 K approach 9.90 N β which is very close to the expected spin-only value of 10 N β . Likewise, the χT value of 8.86 cm³ K mol⁻¹ at 250 K is in accord with the expected 8.75 cm³ K mol⁻¹ value for two non-interacting $g = 2.0 \text{ Mn}^{\text{II}}$ centres. The decrease in $\chi T vs. T$ below 20 K is attributed to weak antiferromagnetic interactions through the diamagnetic [Re^{III}(CN)₇]⁴⁻ linker. AC magnetic susceptibility measurements for this compound did not reveal any out-of-phase signal down to 1.8 K. Synthesis of mixed Mo^{III}/Re^{III} systems based on these findings is in progress.

Conclusions

Four new 3-D coordination networks based on Mn^{II} units and $[Mo^{III}(CN)_7]^{4-}$ were obtained and their magnetic ordering temperatures and coercivities were correlated with the connectivity patterns, metrical parameters and the geometry of the heptacyanomolybdate(III) anion. The collective results support the hypothesis that the pentagonal bipyramidal geometry leads to significant magnetic anisotropy and wide magnetic hysteresis loops. Importantly, it was found that the presence of equatorial cyanide bridges does not suppress magnetic hysteresis in 1–3. Moreover, it appears that the Mn–N–C angles in 1–4 are important for obtaining hard magnetic materials with $[Mo(CN)_7]^{4-}$ building blocks, although the current study is too limited to warrant specific conclusions in this regard.

Reactions of the diamagnetic [Re^{III}(CN)₇]⁴⁻ anion⁴³ that involve substitution of $[Mo^{III}(CN)_7]^{4-}$ in $\{[Mn^{II}(L)_x(H_2O)_y]_2[Mo^{III}(CN)_7]\}$. nH₂O compounds are promising avenues of investigation as evidenced by the fact that the 3-D Mn^{II}-[Re^{III}(CN)₇] analogue, 1Re, was successfully isolated in this study. This paramagnetic framework solid, the first example of a bimetallic coordination framework based on the heptacyanorhenate(III) anion, is isomorphous to its ferrimagnetically ordered heptacyanomolybdate(III) analogue, a fact that bodes well for successful magnetic dilution of the Mn^{II}-Mo^{III} networks. 44 Partial, rather than complete, substitution of the paramagnetic heptacyanomolybdate(III) anion in these networks could lead to SMM-like slow paramagnetic relaxation, as, for example, in lanthanidebased networks 45,46 such as Dy_{0.06}Y_{0.94}(OH)CO₃ which exhibits a spin-reversal barrier as high as 196(6) K in a zero DC field.⁴⁷ Analogous studies for transition metal-based frameworks have not been undertaken, however, and are worth pursuing; work in this vein is in progress.

Conflicts of interest

There are no conflicts to declare.

Acknowledgements

This work was financed by the Polish National Science Centre within the Sonata Bis 6 (2016/22/E/ST5/00055) research project. KRD is grateful to the National Science Foundation (CHE-1808779) and the Robert A. Welch Foundation under Grant Number A-1449 for financial support.

Notes and references

- 1 A. Kraft, Bull. Hist. Chem., 2008, 33, 61-67.
- 2 A. N. Holden, B. T. Matthias, P. W. Anderson and H. W. Lewis, *Phys. Rev. B*, 1956, **102**, 1463.
- 3 B. Mayoh and P. Day, *Chem. Soc., Dalton Trans.*, 1976, 1483–1486.

- 4 M. B. Robin and P. Day, Adv. Inorg. Chem. Radiochem., 1968, 10, 247.
- 5 B. Sieklucka and D. Pinkowicz, *Molecular Magnetic Materials: Concepts and Applications*, Wiley, 2017.
- 6 S. Ferlay, T. Mallah, R. Ouahès, P. Veillet and M. Verdaguer, *Nature*, 1995, **378**, 701.
- 7 S. M. Holmes and G. S. Girolami, J. Am. Chem. Soc., 1999, 121, 5593.
- 8 B. Sieklucka, R. Podgajny, P. Przychodzeń and T. Korzeniak, *Coord. Chem. Rev.*, 2005, **249**, 2203.
- 9 Y. Arimoto, S.-I. Ohkoshi, Z. J. Zhong, H. Seino, Y. Mizobe and K. Hashimoto, *J. Am. Chem. Soc.*, 2003, **125**, 9240.
- 10 J. Larionova, J. Sanchiz, S. Gohlen, L. Ouahab and O. Kahn, *Chem. Commun.*, 1998, 953.
- 11 J. Larionova, R. Clérac, J. Sanchiz, O. Kahn, S. Golhen and L. Ouahab, *J. Am. Chem. Soc.*, 1998, **120**, 13088.
- 12 J. Larionova, O. Kahn, S. Golhen, L. Ouahab and R. Clérac, *Inorg. Chem.*, 1999, 38, 3621.
- 13 O. Kahn, J. Larionova and L. Ouahab, *Chem. Commun.*, 1999, 945.
- 14 J. Larionova, O. Kahn, S. Gohlen, L. Ouahab and R. Clérac, J. Am. Chem. Soc., 1999, 121, 3349.
- 15 J. Larionova, R. Clérac, B. Donnadieu and C. Guérin, *Chem. Eur. J.*, 2002, **8**, 2712.
- 16 A. K. Sra, F. Lahitite, J. V. Yakhmi and O. Kahn, *Phys. B*, 2002, 321, 87.
- 17 S. Tanase, F. Tuna, P. Guionneau, T. Maris, G. Rombaut, C. Mathonière, M. Andruh, O. Kahn and J.-P. Sutter, *Inorg. Chem.*, 2003, **42**, 1625.
- 18 X. F. Le Goff, S. Willemin, C. Coulon, J. Larionova, B. Donnadieu and R. Clérac, *Inorg. Chem.*, 2004, 43, 4784.
- 19 K. Tomono, Y. Tsunobuchi, K. Nakabayashi and S.-i. Ohkoshi, *Inorg. Chem.*, 2010, **49**, 1298.
- 20 L. Shi, D. Shao, F.-Y. Shen, X.-Q. Wei and X.-Y. Wang, *Chin. J. Chem.*, 2018, 37, 19.
- 21 J. Milon, P. Guionneau, C. Duhayon and J.-P. Sutter, *New J. Chem.*, 2011, 35, 1211.
- 22 J. Milon, M.-C. Daniel, A. Kaiba, P. Guionneau, S. Brandès and J.-P. Sutter, *J. Am. Chem. Soc.*, 2007, **129**, 13872.
- 23 X.-Y. Wang, A. V. Prosvirin and K. R. Dunbar, *Angew. Chem.*, *Int. Ed.*, 2010, **49**, 5081.
- 24 K. Qian, X.-C. Huang, C. Zhou, X.-Z. You, X.-Y. Wang and K. R. Dunbar, *J. Am. Chem. Soc.*, 2013, 135, 13302.
- 25 D.-Q. Wu, D. Shao, X.-Q. Weri, F.-X. Shen, L. Shi, D. Kempe, Y.-Z. Zhang, K. R. Dunbar and X.-Y. Wang, *J. Am. Chem. Soc.*, 2017, 139, 11714.
- 26 D. Gatteschi, R. Sessoli and J. Villain, *Molecular Nanomagnets*, Oxford University Press, 2006.
- 27 V. S. Mironov, L. F. Chibotaru and A. Ceulemans, *J. Am. Chem. Soc.*, 2003, **125**, 9750.
- 28 V. S. Mironov, Inorg. Chem., 2015, 54, 11339.
- 29 V. S. Mironov, Inorganics, 2018, 6, 58.
- 30 L. F. Chibotaru, M. F. A. Hendrickx, S. Clima, J. Larionova and A. Ceulemans, *J. Phys. Chem. A*, 2005, **109**, 7251.
- 31 X.-Q. Wei, K. Qian, H.-Y. Wei and X.-Y. Wang, *Inorg. Chem.*, 2016, 55, 5107.

32 R. C. Young, J. Am. Chem. Soc., 1932, 54, 1402.

Paper

- 33 W. P. Griffith, P. M. Kiernan and J.-M. Brégeault, *J. Chem. Soc.*, *Dalton Trans.*, 1978, 1411.
- 34 D. Pinkowicz, R. Podgajny, W. Nitek, M. Makarewicz, M. Czapla, M. Mihalik, M. Bałanda and B. Sieklucka, *Inorg. Chim. Acta*, 2008, 361, 3957.
- 35 L. Shen, Y. Zhang and J. Uiu, J. Coord. Chem., 2006, 59, 629.
- 36 M. Magott, M. Reczyński, B. Gaweł, B. Sieklucka and D. Pinkowicz, *J. Am. Chem. Soc.*, 2018, **140**, 15876.
- 37 X.-Q. Wei, Q. Pi, F.-X. Shen, D. Shao, H.-Y. Wei and X.-Y. Wang, *Dalton Trans.*, 2018, 47, 11873.
- 38 Q.-L. Wang, H. Southerland, J.-R. Li, A. V. Prosvirin, H. Zhao and K. R. Dunbar, *Angew. Chem., Int. Ed.*, 2012, **51**, 9321.
- 39 Q.-L. Wang, Y.-Z. Zhang, H. Southerland, A. V. Prosvirin, H. Zhao and K. R. Dunbar, *Dalton Trans.*, 2014, 43, 6802.
- 40 M. Llunell, D. Casanova, J. Cirera, P. Alemany and S. Alvarez, *SHAPE v. 2.1, 2013*, University of Barcelona, Barcelona, Spain.

- 41 G. R. Rossman, F.-D. Tsay and H. B. Gray, *Inorg. Chem.*, 1973, 12, 824.
- 42 N. F. Chilton, R. P. Anderson, L. D. Turner, A. Soncini and K. S. Murray, *J. Comput. Chem.*, 2013, 34, 1164.
- 43 P. M. Kiernan and W. P. Griffith, *Inorg. Nucl. Chem. Lett.*, 1976, 12, 377.
- 44 P. Konieczny, R. Pełka, T. Wasiutyński, M. Oszajca, B. Sieklucka and D. Pinkowicz, *Dalton Trans.*, 2018, 47, 11438.
- 45 R. Giraud, W. Wernsdorfer, A. M. Tkachuk, D. Mailly and B. Barbara, *Phys. Rev. Lett.*, 2001, **87**, 057203.
- 46 B. Monteiro, J. T. Coutinho, C. C. L. Pereira, L. C. J. Pereira, J. Marçalo, M. Almeida, J. J. Baldovi, E. Coronado and A. Gaita-Ariño, *Inorg. Chem.*, 2015, 54, 1949.
- 47 J. Liu, Y.-C. Chen, J.-J. Lai, Z.-H. Wu, L.-F. Wang, Q.-W. Li, G.-Z. Huang, J.-H. Jia and M.-L. Tong, *Inorg. Chem.*, 2016, 55, 3145.